

Synthesis, Crystal Structure and Characterizations of the Perovskite-Type ScRh_3B_x Compounds

Shigeru OKADA*¹, Toetsu SHISHIDO*² and Kunio KUDOU*³

Abstract: Polycrystalline samples of ScRh_3B_x , which consists of highly reactive Sc and high melting point Rh and B elements, have been successfully synthesized by arc-melting method. Compound of ScRh_3B_x has perovskite type cubic structure (space group: $Pm\bar{3}m$). The nonstoichiometric perovskite-type ScRh_3B_x exists in the homogeneity range of $0 \leq x \leq 1.00$. Lattice parameter of a in annealed ScRh_3B_x depends on x , and varies linearly from $a=0.3903(1)$ nm ($x=0$) to $a=0.4080(1)$ nm ($x=1.00$). The micro-Vickers hardness and electrical resistivity of the compounds were measured, and oxidation at high-temperature in air was studied. Average values of micro-Vickers hardness and electrical resistivity determined on ScRh_3B_x compounds are as follows: for $\text{ScRh}_3\text{B}_{1.000}$: $9.9(\pm 0.1)$ GPa, 43.9×10^{-6} Ωcm ; for $\text{ScRh}_3\text{B}_{0.210}$: $4.6(\pm 0.05)$ GPa, 34.4×10^{-6} Ωcm ; for ScRh_3 : $1.9(\pm 0.1)$ GPa, 18.0×10^{-6} Ωcm . All samples in the range of $0 \leq x \leq 1.00$ show the metallic temperature dependence of the resistivity down to 0.5 K. Magnetic susceptibilities also show the Pauli paramagnetic behaviour and no trace of the magnetic transitions and superconductivity in all samples. The oxidation reaction of $\text{ScRh}_3\text{B}_{1.000}$, $\text{ScRh}_3\text{B}_{0.210}$, and ScRh_3 compounds in air starts at about 595°C , 702°C , and 415°C , respectively, and final weight gains were found to be in the range from about 5.8 to 12.7 wt%. The identified oxidation product consisted from the Sc_2O_3 , Rh and ScBO_3 .

Keyword: ScRh_3B_x , Perovskite-type, Arc-melting method, Crystal structure, Micro-Vickers hardness, Electrical resistivity, Magnetic property, Oxidation property

1. Introduction

The rare earth elements (RE)-platinum group elements-boron (B) ternary system have interesting behavior in magnetism and superconductivity^{1,2}. In the ternary RE-Rh-B system, RERh_3B , RERh_3B_2 , and RERh_4B_4 are reported. Rare earth rhodium borides RERh_3B with perovskite cubic structure (space group: $Pm\bar{3}m$) have been investigated many researchers³⁻⁵. They are ErRh_3B (cubic system, space group: $Pm\bar{3}m$, $a=0.4146$ nm), ErRh_3B_2 (base-centered monoclinic system, ErIr_3B_2 type, space group: $C2/m$, $a=0.5355(1)$ nm, $b=0.9282(1)$ nm, $c=0.3102(1)$ nm, $\beta=90.89(3)^\circ$), and ErRh_4B_4 (simple tetragonal system, space group: $P4_2/nmc$, $a=0.5304(1)$ nm, $c=0.7395(2)$ nm). The magnetic and superconducting properties of these crystals have been reported. We have prepared

LaRh_3B , GdRh_3B , and LuRh_3B using arc-melting. The B deficient compounds, RERh_3B_x can be obtained. The B content variation induces the varies properties such as electro-magnetism, microhardness, and chemical resistance against to oxidation in air at high temperature⁶⁻⁸.

Recently we have been synthesized polycrystalline ScRh_3B_x compounds by the arc-melting method using high reactive (Sc) and high melting (Rh, B) elements⁹. However, there is a little information about chemical and physical properties of ScRh_3B .

The purpose of this paper is to clarify the homogeneity range of the nonstoichiometric perovskite-type ScRh_3B_x compounds from the X-ray diffraction and chemical analyses. Crystallographic data, micro-Vickers hardness, electrical resistivity, and oxidation resistivity at high temperature in air of these compounds were studied.

2. Experimental details

Samples of ScRh_3B_x compounds were synthesized by arc-melting method using Sc metal chips (purity 99.9%), Rh powder (purity 99.9%) and crystalline B powder (purity 99.9%) as raw materials. They were weighed in the atomic ratio 1:3: x , where $x=1.333$ (25 at.%), 1.000 (20 at.%), 0.706 (15 at.%), 0.444 (10 at.%), 0.210 (5 at.%), and 0. The mixture of the starting materials, about 2 g of each sample, were placed in a water-cooled copper hearth

*¹ 工学部土木工学科 助教授 工学博士

Department of Civil Engineering, Faculty of Engineering, Associate Professor, Dr. of Engineering

*² 東北大学 金属材料研究所 新素材設計開発施設結晶作製研究ステーション 助教授 工学博士

Institute for Materials Research, Tohoku University, Associate Professor, Dr. of Engineering

*³ 神奈川大学 工学部機械工学科 助手 博士 (工学)

Department of Mechanical Engineering, Faculty of Engineering, Kanagawa University, Research Associate, Dr. of Engineering

in a reaction chamber (Model DAIA-ACM-01). Fig. 1 shows the schematic arrangement of the reaction chamber. The pressure inside the reaction chamber was approximately 1.33×10^{-5} Pa. A small amount of residual oxygen in argon was eliminated by fusion a button of titanium as a reducing reagent. The starting materials were then melted by an argon arc plasma flame. The flame was maintained under the conditions of DC 20 V and 100 A. The samples (turned over) were melted three times for 3 min each. Finally synthesized samples were wrapped in tantalum foil and annealed at 1300°C for 24 h under vacuum to ensure homogeneity.

For chemical analysis, the samples were fused using NaHSO_4 as a flux, then the obtained material was dissolved in hydrochloric acid. The chemical composition of each solution was analyzed by the induction coupled plasma atomic emission spectrometry (ICP-AES) method, using Zn as internal standard. Phase analysis and determination of the lattice parameters were performed using a powder X-ray diffractometer (XRD) with monochromatic $\text{CuK}\alpha$ radiation ($\lambda=0.15418$ nm) at room temperature. The samples synthesized were cut with a diamond cutter

and polished to obtain mirror surfaces. These surfaces were investigated by a scanning electron microscope (SEM), an electron probe micro-analyzer (EPMA), and an energy-dispersive detector (EDX). The Vickers microhardness (Hv) for the samples was measured at room temperature in air. With the use of a diamond pyramid having an apex angle of 136° , the samples were pressed by the pressure load of 0.245 N to 9.800 N for 15 s at about 6–8 points for the mirror surfaces of each crystal. The values obtained were averaged and the experimental error was estimated. The electrical resistivities of the crystals measured by a direct-current four-probe technique at room temperature in air. Thermogravimetric (TG) analysis and differential thermal analysis (DTA) were performed between room temperature and 1200°C to study the oxidation resistivity of the samples in air. A sample of about 25 mg to 30 mg was heated at a rate of $10^\circ\text{C min}^{-1}$ to 1200°C. The oxidation products were analyzed by XRD.

3. Results and discussion

3.1 Synthesis of ScRh_3B_x compounds

Polycrystalline samples of ScRh_3B_x , which consists of

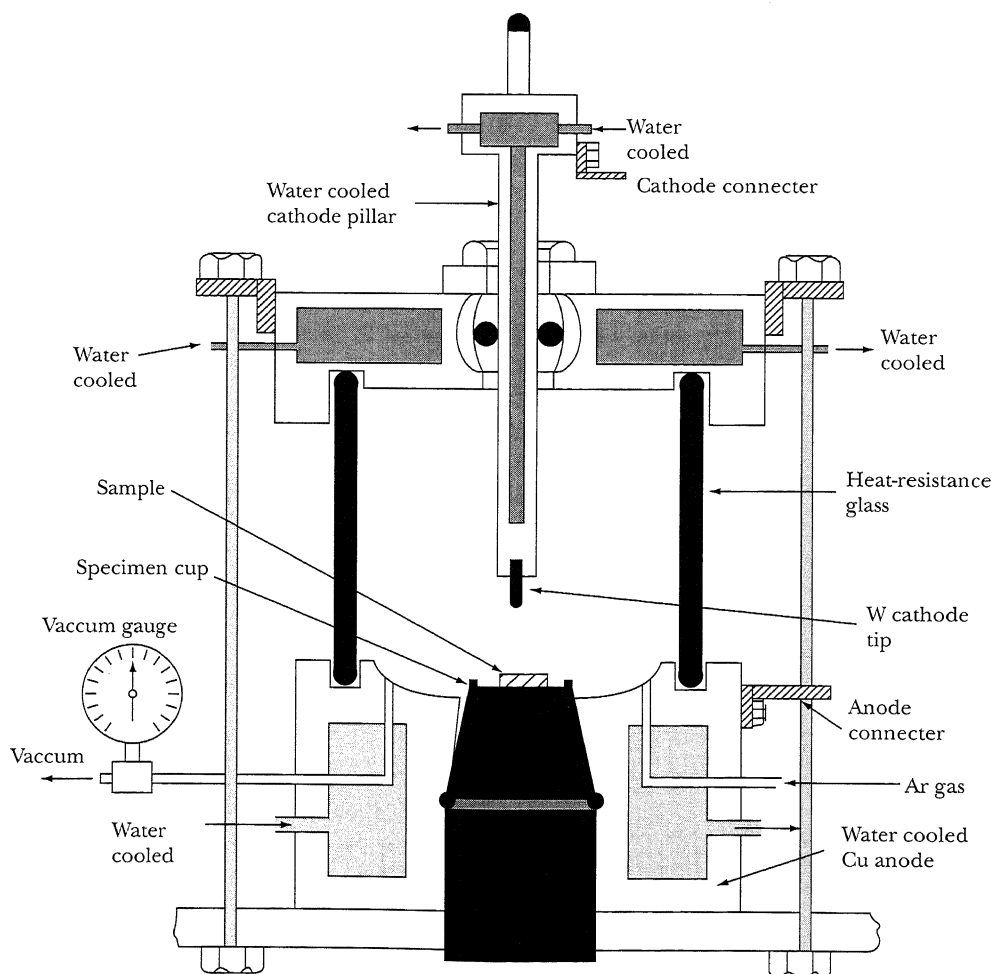


Fig. 1 The argon arc furnace (simplified).

highly reactive Sc and high melting point Rh and B elements, have been successfully synthesized by arc-melting method. All the synthesized samples revealed a silvery metallic luster. The mixture of the starting materials, and the results of the chemical analyses for the synthesized ScRh_3B_x are listed in Table 1. According to chemical analyses, the chemical compositions of the obtained samples almost corresponded to the atomic ratio of the starting compositions. No evidence was obtained of pollution from the electrodes or the hearth by the arc-melting method.

3.2 Solid solution range of boron

The relation between composition and structure of ScRh_3B_x ($0 \leq x \leq 1.333$) were determined. The stoichiometric composition of ScRh_3B_x belongs to the cubic system and is a perovskite type (space group $Pm\bar{3}m$). The crystal structure of ScRh_3B is illustrated in Fig. 2. As seen from

Table 1 Results of the chemical analyses for the synthesized ScRh_3B_x

Nominal composition (atomic% of B)	Results of the chemical analyses, weight% (nominal composition, weight%)	Results of the chemical analyses, weight%		
		Sc	Rh	B
$\text{ScRh}_3\text{B}_{1.333}$ (25)	12.46 (12.49)	84.02 (84.15)	2.99 (3.04)	
$\text{ScRh}_3\text{B}_{1.000}$ (20)	12.64 (12.68)	84.54 (84.58)	2.33 (2.39)	
$\text{ScRh}_3\text{B}_{0.706}$ (15)	12.72 (12.68)	85.52 (85.22)	1.38 (1.61)	
$\text{ScRh}_3\text{B}_{0.444}$ (10)	12.88 (13.00)	85.62 (85.94)	0.90 (0.78)	
$\text{ScRh}_3\text{B}_{0.210}$ (5)	12.80 (12.72)	86.87 (86.53)	0.48 (0.47)	
ScRh_3 (0)	12.78 (12.93)	86.70 (86.55)	—	

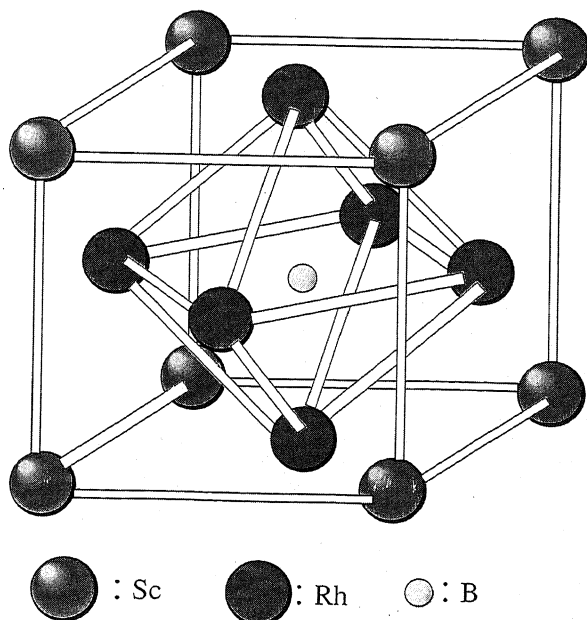


Fig. 2 The crystal structure of ScRh_3B compound.

Fig. 2, the Sc positioned at the eight corners of the cube, Rh at the centers of the six faces, and boron at the body center of the cube. Fig. 3 shows the XRD patterns for samples of ScRh_3B_x . In the case of $x=1.333$, impurity phase coexists with the perovskite type phase. From the result of the powder XRD analysis for ScRh_3B_x , the amount of the impurity phase increases as the concentration of boron increases, it can be concluded that the perovskite-type compounds exist in the range of $0 \leq x \leq 1.000$ (0 to 20 at. %). The solid solution ranges of boron in ScRh_3B_x are no agreement with those reported for ErRh_3B_x ⁹ and HoRh_3B_x ¹⁰. In the case of $x=0$, ScRh_3 has AuCu_3 type structure, its space group is also $Pm\bar{3}m$. ScRh_3B_x exists in the range of $0 \leq x \leq 1.000$ (0 to 20 at. %). Fig. 4 shows the variation of lattice parameter a as a function of boron concentration x in the cubic structure ScRh_3B_x . The lattice parameters expands with an increasing concentration of boron in the compound. The lattice parameter a in annealed depends on x , and varies linearly from

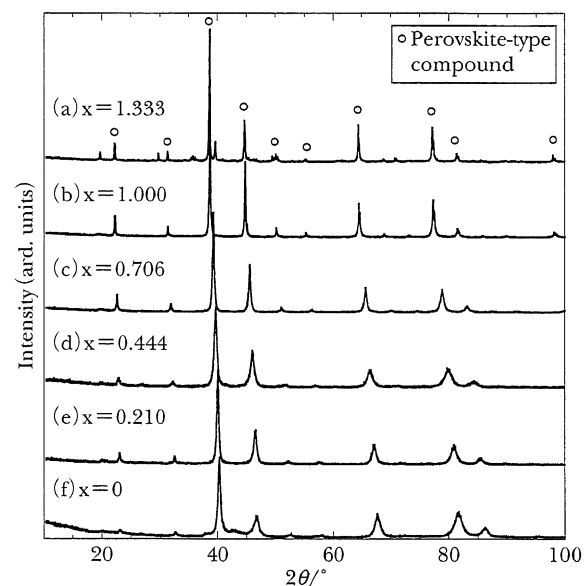


Fig. 3 X-ray diffraction patterns for ScRh_3B_x .

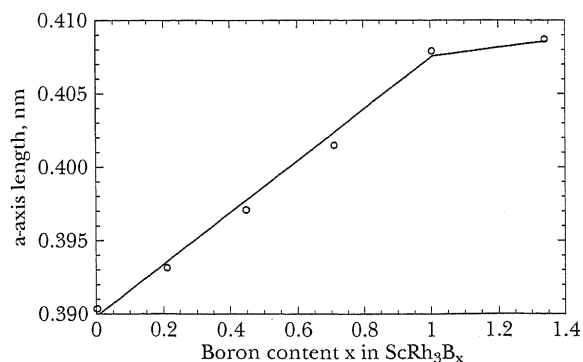


Fig. 4 Relationships between boron content x in ScRh_3B_x and a -axis length.

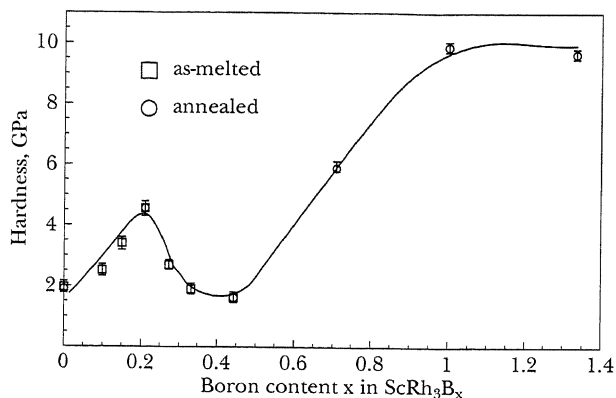


Fig. 5 Relationships between boron content x in ScRh_3B_x and microhardness.

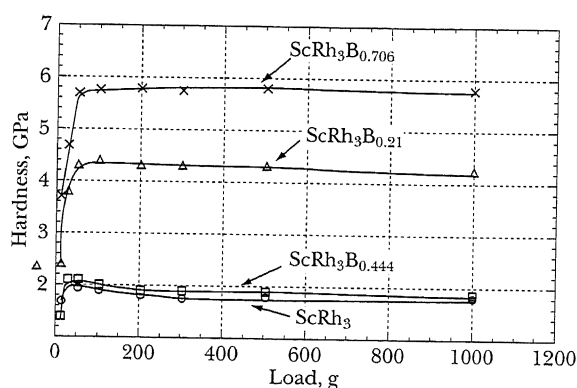


Fig. 6 Relationships between boron content x in ScRh_3B_x and load-dependency of Vickers microhardness.

$a=0.3903(1)$ nm ($x=0$) to $a=0.4080(1)$ nm ($x=1.000$). ScRh_3B_x compounds supports the view that the solid solution range of boron in $0 \leq x \leq 1.000$ (0 to 20 at. %).

3.3 Microhardness and electrical resistivity

The Vickers microhardness of ScRh_3B_x compounds ($0 \leq x \leq 1.000$) were measured in several directions. As listed in Fig. 5, Fig. 6 and Table 2, the value of the Vickers microhardness for ScRh_3B_x are distributed from $1.9(\pm 0.1)$ GPa to $9.9(\pm 0.1)$ GPa. The hardness increases as the boron content increases in a range between ScRh_3

Table 2 Micro-Vickers hardness and electrical resistivity at 20°C of ScRh_3B_x compounds

Sample Starting composition (mol% of boron)	Microhardness* (GPa)	Electrical resistivity ($\times 10^{-6}$, Ωcm)
$\text{ScRh}_3\text{B}_{1.000}$ (20)	$9.9 (\pm 0.1)$	43.9
$\text{ScRh}_3\text{B}_{0.706}$ (15)	$5.9 (\pm 0.05)$	22.4
$\text{ScRh}_3\text{B}_{0.444}$ (10)	$1.6 (\pm 0.1)$	26.3
$\text{ScRh}_3\text{B}_{0.210}$ (5)	$4.6 (\pm 0.05)$	34.4
ScRh_3 (0)	$1.9 (\pm 0.1)$	18.0

* Load; 2.94 N, Load time; 15 sec.

$\text{B}_{1.000}$ and $\text{ScRh}_3\text{B}_{0.706}$. Apparent minimums in hardness are found at $\text{ScRh}_3\text{B}_{0.444}$ and ScRh_3 . This result suggests that the hardness of the boride essentially depends on the boron content in the compound.

The electrical resistivity are listed in Table 2. The electrical resistivity of the annealed ScRh_3B_x compounds is in the range of $18.0 \times 10^{-6} \Omega\text{cm}$ ($x=0$) $\sim 43.9 \times 10^{-6} \Omega\text{cm}$ ($x=1.000$).

3.4 Oxidation resistance in air

Fig. 7. shows TG-DTA curves for ScRh_3B_x compounds. According to the DTA analysis, one or two exothermic peaks was observed. The maximum temperature for the exothermic peak is 856°C . The oxidation reaction of $\text{ScRh}_3\text{B}_{1.000}$, $\text{ScRh}_3\text{B}_{0.706}$, $\text{ScRh}_3\text{B}_{0.444}$, $\text{ScRh}_3\text{B}_{0.210}$, and ScRh_3 compounds in air starts at about 595°C , 583°C , 685°C , 702°C , and 415°C , respectively. Mixed phase of Rh plus Sc_2O_3 and ScBO_3 is identified as an oxidized product. In all cases, a B_2O_3 phase was not detected by XRD. Oxidation onset temperature, weight gain and oxidation product from TG-DTA measurements for the ScRh_3B_x compounds are summarized in Table 3. Hence oxidation resistivity of ScRh_3 is relatively low.

4. Conclusion

Polycrystalline ScRh_3B_x compounds were prepared from arc-melting method using Sc, Rh and B elements. The authors can draw the following conclusion from this study.

Table 3 Results of the chemical analyses for the synthesized ScRh_3B_x , and phenomenal temperature from TG-DTA measurement on ScRh_3B_x

Sample nominal composition (atomic% of boron)	Oxidation onset ($^\circ\text{C}$) by TG	Exotherm maximum ($^\circ\text{C}$) by DTA	Weight gain (%)	Oxidized products by XRD
$\text{ScRh}_3\text{B}_{1.333}$ (25)	599	780	12.6	Rh, Sc_2O_3 , ScBO_3
$\text{ScRh}_3\text{B}_{1.000}$ (20)	595	797	12.7	Rh, Sc_2O_3 , ScBO_3
$\text{ScRh}_3\text{B}_{0.706}$ (15)	583	766, 812	10.8	Rh, Sc_2O_3 , ScBO_3
$\text{ScRh}_3\text{B}_{0.444}$ (10)	685	828	7.8	Rh, Sc_2O_3 , ScBO_3
$\text{ScRh}_3\text{B}_{0.210}$ (5)	702	742, 856	5.8	Rh, Sc_2O_3
ScRh_3 (0)	415	719	7.2	Rh, Sc_2O_3

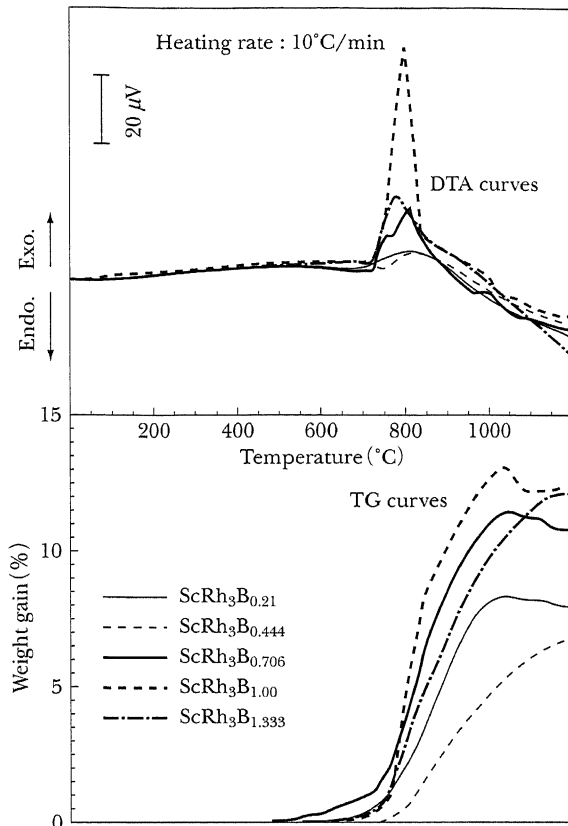


Fig. 7 TG-DTA curves for ScRh_3B compounds.

- (1) The nonstoichiometric perovskite-type ScRh_3B_x exists in the homogeneity range of $0 \leq x \leq 1.00$.
- (2) The lattice parameter a in annealed ScRh_3B_x depends on x and varies linearly from $a=0.3903(1)$ nm ($x=0$) to $a=0.4080(1)$ nm ($x=1.00$).
- (3) The micro-Vickers hardness of the annealed ScRh_3B_x increases with increasing B content in the range $x=0$ – 1.000 , from $1.9(\pm 0.1)$ GPa to $9.9(\pm 0.1)$ GPa.
- (4) The electrical resistivity of the annealed ScRh_3B_x is in

the range of $18.0 \times 10^{-6} \Omega\text{cm}$ ($x=0$) \sim $43.9 \times 10^{-6} \Omega\text{cm}$ ($x=1.000$).

(5) The oxidation reaction of $\text{ScRh}_3\text{B}_{1.000}$, $\text{ScRh}_3\text{B}_{0.706}$, $\text{ScRh}_3\text{B}_{0.444}$, $\text{ScRh}_3\text{B}_{0.210}$, and ScRh_3 compounds in air starts at about 595°C , 583°C , 685°C , 702°C , and 415°C , respectively. The sample changed to Rh, Sc_2O_3 and ScBO_3 after oxidation.

Acknowledgments

The present study was performed under the cooperative research program of the IMR, Tohoku University. The authors wish to thank Dr. K. Iizumi and Dr. M. Ogawa of Tokyo Institute of Polytechnics for help in the experiments.

(Received September 28, 2000)

References

- 1) M. Hakimi, J. G. Huber, S. K. Dhar, S. K. Malik, J. Less-Common Metal., **94**, 157 (1983).
- 2) J. Bernhard, I. Higashi, P. Granberg, L.-E. Terenius, T. Lundström, T. Shishido, A. Rukolainen, H. Takei, T. Fukuda, J. Alloys Comp., **193** (1993) 295.
- 3) P. Rogl, L. Delong, J. Less-Common Metals, **91** (1983) 97.
- 4) H. Takei, T. Shishido, J. Less-Common Metals, **97** (1984) 223.
- 5) T. Shishido, I. Higashi, H. Kitazawa, J. Bernhard, H. Takei, T. Fukuda, Jpn. J. Appl. Phys., Series 10, Boron, Borides and Related Compounds, (1994) 142.
- 6) T. Shishido, J. Ye, K. Kudou, S. Okada, K. Obara, T. Sugawara, M. Oku, K. Wagatsuma, H. Horiuchi, T. Fukuda, J. Alloys Comp., **291** (1999) 52.
- 7) T. Shishido, J. Ye, K. Kudou, S. Okada, A. Yoshikawa, H. Horiuchi, T. Fukuda, J. Ceram. Soc. Japan, **107** [6] 546 (1999) (in Japanese).
- 8) T. Shishido, J. Ye, K. Kudou, S. Okada, M. Oku, A. Yoshikawa, H. Horiuchi, T. Fukuda, J. Ceram. Soc. Japan, **108** [7] 683 (2000) (in Japanese).
- 9) S. Okada, K. Kudou, T. Shishido, Y. Sato, T. Fukuda, Jpn. J. Appl. Phys., **35** (1996) L790.
- 10) T. Shishido, M. Oku, T. Sasaki, H. Iwasaki, H. Kishi, H. Horiuchi, T. Fukuda, J. Alloys Comp., **283** (1999) 91.